Research Article | Vol. 29, No. 21 / 11 Oct 2021 / Optics Express 34066
Optics EXPRESS

Improved optical camera communication systems using a freeform lens

ZIWEI LIU,[1] LIN YANG,[2] YANBING YANG,[1,3,6] RENGMAO WU,[2,7] LEI ZHANG,[1,3] LIANGYIN CHEN,[1,3] DIE WU,[4] AND JUN SHE[5]

[1]College of Computer Science, Sichuan University, Chengdu 610065, China
[2]State key Laboratory of Modern Optical Instrumentation, College of Optical Science and Engineering, Zhejiang University, Hangzhou 310058, China
[3]Institute for Industrial Internet Research, Sichuan University, Chengdu 610065, China
[4]School of Computer Science, Sichuan Normal University, Chengdu 610066, China
[5]YEJIA Optical Technology (Guangdong) Corporation, Block B, No. 2 Longpu Road, Tangxia, Dongguan, Guangdong 523715, China
[6]yangyanbing@scu.edu.cn
[7]wrengmao@zju.edu.cn

Abstract: Optical camera communication (OCC) systems, which utilize image sensors embedded in commercial-off-the-shelf devices to detect time and spatial variations in light intensity for enabling data communications, have stirred up researchers' interest. Compared to a direct OCC system whose maximum data rate is strongly determined by the LED source size, a reflected OCC system can break that limitation since the camera captures the light rays reflecting off an observation plane (e.g., a wall) instead of those light rays directly emanated from the light source. However, the low signal-to-noise ratio caused by the non-uniform irradiance distribution produced by LED luminaire on the observation plane in current reflected OCC systems cannot be avoided, hence low complexity and accurate demodulation are hard to achieve. In this paper, we present a FreeOCC system, which employs a dedicatedly tailored freeform lens to precisely control the propagation of modulated light. A desired uniform rectangular illumination is produced on the observation plane by the freeform lens, yielding a uniform grayscale distribution within the received frame captured by the camera in the proposed FreeOCC system. Then, the received signal can be easily demodulated with high accuracy by a simple thresholding scheme. A prototype of the FreeOCC system demonstrates the high performance of the proposed system, and two pulse amplitude modulation schemes (4-order and 8-order) are performed. By using the freeform lens, the packet reception rate is increased by 35% and 32%, respectively; the bit error rate is decreased by 72% and 59%, respectively, at a transmission frequency of 5 kHz. The results clearly show that the FreeOCC system outperforms the common reflected OCC system.

1. Introduction

Optical camera communication (OCC) is a prominent technology, which can reuse the pervasively deployed LED lighting infrastructures and cameras to realize ubiquitous data communication [1–3]. Limited by the low frame rate of cameras, the earlier works of OCC can only achieve a very low data rate of several bytes per second [4,5]. To break the frame rate limitation, the seminal approach of [6] proposes to leverage the rolling shutter effect of a complementary metal-oxide-semiconductor (CMOS) camera to capture the modulated light for communication and boosts the data rate to kilobits per second. A rolling shutter camera, instead of exposing the image frame at once, conducts the exposure in a column-by-column (or row-by-row) manner, so the received frame yields dark or bright bands according to the on or off status of the LED transmitters [7,8]. Therefore, a frame can normally carry more than tens of bits (bands), and this allows the OCC system to have a high data rate much greater than its frame rate [9]. Besides, the

#440342 https://doi.org/10.1364/OE.440342
Journal © 2021 Received 12 Aug 2021; revised 23 Sep 2021; accepted 24 Sep 2021; published 4 Oct 2021

Optics EXPRESS

OCC also has several notable benefits, including abundant and unregulated spectrum, link-level security, and easy availability. Due to these unique merits, the OCC systems have been widely investigated [10–14].

The current OCC systems can be grouped into two types: direct OCC and reflected OCC systems [7,10,15,16]. In a direct OCC system, the camera is placed facing the LED transmitter and captures the light rays directly emanated from the light source. Although this configuration could yield a high signal-to-noise ratio (SNR), its maximum data rate is strongly determined by the LED luminaire size, because only the projection area [region of interest (RoI)] of the LED luminaire contains valid data bits in the received frames. Due to the nature of the direct OCC systems, we may need a huge LED light source with a source size similar to that of a conventional fluorescent tube to obtain a data rate at a kbit/s level at a reasonable working distance [8,16]. In a reflected OCC system, the camera is placed facing an observation plane (e.g., a wall) and captures the light rays reflecting off the observation plane. The maximum data rate of a reflected OCC system is hence determined by the size of the illuminated observation plane instead of the LED luminaire size. Since the illumination region size is normally much greater than the LED luminaire size, so the maximum data rate of a reflected OCC system could be much greater than that of a direct OCC system [16]. But the light rays after reflecting off the observation plane are captured by the camera of a reflected OCC system, inevitably the reflected OCC systems are facing a big challenge: a non-uniform irradiance distribution on the observation plane leading to a low SNR in the received frames. Specifically, a non-uniform illumination pattern on the observation plane produced by the LED luminaire yields a higher grayscale at the center and a gradual decrease in grayscale on both sides (shown in Fig. 1). Consequently, the SNR in the marginal region of the frame is much lower than that in the central region, which complicates the demodulation procedure and seriously degrades the communication performance.

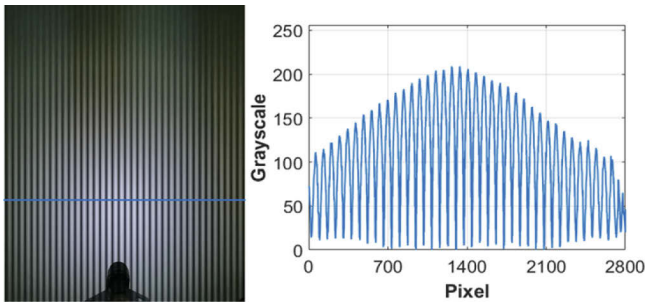

Fig. 1. A non-uniform illumination yields a non-uniform grayscale distribution captured by the camera in a reflected OCC system.

To alleviate the impact caused by the non-uniform SNR and increase the accuracy of demodulation, several methods have been proposed in prior works. An early method suggests using polynomial regression to fit the change of grayscale [6]. From the perspective of signal enhancement, some methods explore to leverage modified algorithms to restore the damaged pixels in the received frames and transform the grayscale levels with high uniformity [17,18]. Focusing on frame processing, a technique that extracts signals with nearly uniform amplitude in received frames to ameliorate the non-uniformity of the received signal is proposed in [19]. Furthermore, other techniques have also been explored, such as entropy-based [20] and pixel-boundaries-based algorithms [21] to combat the non-uniform SNR in reflected OCC. However, it is important to highlight that all these methods above perform with high computational resource consumption and cannot be suitable for energy and computation-limited mobile devices. Taking into account these issues, we suggested a method that improves the reflected OCC communication performance via freeform optic.

Optics EXPRESS

In this paper, we present a FreeOCC system that employs a dedicatedly tailored freeform lens to precisely control the propagation of the modulated light. The freeform lens produces a prescribed uniform rectangular illumination on the observation plane, and the high uniformity of the illumination pattern allows the received signal with uniform and high SNR to be easily demodulated with high accuracy. The rest of the paper is organized as follows. The FreeOCC system will be presented in Section 2, the freeform lens design, signal reception and processing of the proposed FreeOCC system will also be introduced in this section. In Section 3, a prototype of the proposed FreeOCC system will be presented to verify the effectiveness of the proposed system and methods, and elaborate analyses of the prototype will also be made in this section before we conclude our work in Section 4.

2. FreeOCC system

The proposed FreeOCC system is composed of three main components: the freeform transmitter (a LED luminaire employed with the freeform lens), the observation plane (wall), and the receiver (CMOS camera), as shown in Fig. 2. The freeform transmitter uses a field-programmable gate array (FPGA) as the controller to encode input messages and generate modulated signals to the LED light luminaire to emit modulated light. The freeform lens is dedicatedly tailored to precisely control the propagation of the modulated light in tilted geometry. The light rays emanating from the LED luminaire are redirected by the freeform lens to produce a prescribed uniform rectangular illumination on the observation plane which is a white wallpaper attached to a rough wall surface. Thus, the observation plane can be considered as an ideal diffuse reflecting surface. The light rays after refraction by the freeform lens scatter in all directions on the observation plane and some of the scattered rays are subsequently captured by the CMOS camera of a smartphone which is the receiver of the proposed FreeOCC system. The camera extracts the RoI from the received frames, and samples a row of pixels in the RoI to form grayscale sequences. After that, these grayscale sequences captured by camera are stored in text files, and are passed to the PC via a USB for demodulation. In the rest of this section, we will give more physical insights into the designs of the freeform lens, signal reception, and processing of the proposed FreeOCC system.

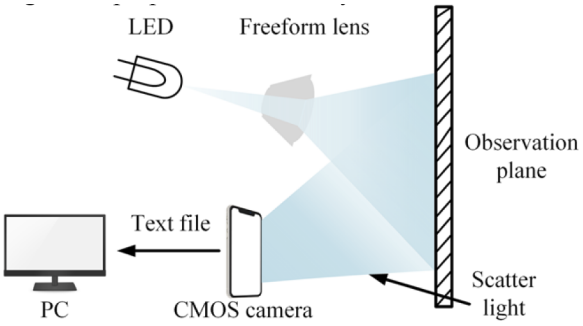

Fig. 2. Illustration of the proposed FreeOCC system.

2.1. Freeform transmitter

In most current reflected OCC systems, the conventional LED luminaires (transmitters) are composed of spherical, parabolic, or ellipsoidal surfaces are used to illuminate the observation plane. Inevitably, the limited control of the modulated light propagation by the conventional LED luminaires leads to a non-uniform illumination pattern on the observation plane, and consequently, the low and non-uniform signal-to-noise ratio in the current reflected OCC systems cannot be avoided. To overcome those limitations of the current reflected OCC systems, a freeform

Optics EXPRESS

transmitter is used in the proposed FreeOCC system, by which the spatial energy distribution of the LED light source is redistributed to produce a uniform rectangular illumination on the target plane. The key that designs a high-performance freeform transmitter is the precise tailoring of the freeform surfaces. However, it is usually not a simple task to perform precise tailoring based on the intensity distribution of the LED light source and the target irradiance distribution. In our recent work [22], we developed a general formulation for designing freeform illumination optics in highly tilted geometry. This method allows us to create high-performance freeform lenses with a flexible geometry of the illumination system. Thus, this method is employed here to design the freeform transmitter in the proposed FreeOCC system. A brief introduction to the design process of the proposed freeform lens is presented below, as shown in Fig. 3.

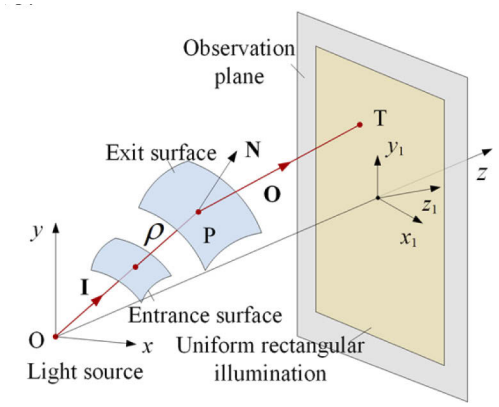

Fig. 3. Geometric layout of the freeform transmitter.

We assume that the entrance surface of the freeform lens is a spherical surface and the exit surface is a freeform surface. The light source is placed at the point O which is the center of curvature of the entrance surface. The origin of the global Cartesian coordinate system is also placed at O with the z-axis parallel to the optical axis of the freeform lens. A local coordinate system is placed at the intersection point of the z-axis and the target plane with the z1-axis perpendicular to the observation plane, as shown in Fig. 3. Since the optical axis is not perpendicular to the observation plane in tilted illumination [22], the z_1-axis in the local coordinate system does not coincide with the z-axis in the global coordinate system. A light ray emanated from the light source passes through the entrance surface and intersects the exit surface at P. Since the LED luminaire is placed at the center of curvature of the spherical entrance surface, the propagation direction of the ray remains unchanged after it passes through the entrance surface. After refraction by the exit surface, the light ray strikes the tilted plane at T. We assume that ρ is the radial distance between S and P, which is a function of the azimuthal angle θ and the polar angle φ. We know that the position vector $\mathbf{P}$ of P can be written as $\mathbf{P}=\rho\times\mathbf{I}$, $\mathbf{I}=(\sin\varphi\cos\theta, \sin\varphi\sin\theta, \cos\varphi)$, which is the unit vector of the incident ray. Then, the unit normal to the exit surface at P is governed by

$$\mathbf{N} = (\mathbf{P}_\varphi \times \mathbf{P}_\theta)/|\mathbf{P}_\varphi \times \mathbf{P}_\theta| \tag{1}$$

where, $\mathbf{P}_\theta$ and $\mathbf{P}_\varphi$ are the tangent vectors of the exit surface at P along with the θ and φ directions. Since the unit vector of the incident ray is known, application of the Snell's law gives us the unit vector $\mathbf{O}$ of the outgoing ray. After simple calculation, we could further obtain the coordinates of T in the local coordinate system. Obviously, the local coordinates of T are functions of ρ_θ, ρ_φ, ρ, θ and φ, which can be written as $t_x=f(\theta,\varphi,\rho,\rho_\varphi,\rho_\theta,)$, $t_y=g(\theta,\varphi,\rho,\rho_\varphi,\rho_\theta,)$, and $t_z=0$. We further assume that the freeform transmitter is lossless, meaning neither Fresnel nor absorption losses are considered here. It means that the energy of an infinitesimal light beam is conserved when

Optics EXPRESS

this infinitesimal light beam passes through the freeform transmitter. Then, the local energy conservation of the infinitesimal light beam can be written as

$$E(t_x, t_y)|\mathrm{J}(\mathbf{T})| - I(\theta, \varphi)\sin\varphi = 0 \tag{2}$$

where, $I(\theta, \varphi)$ is the intensity of the incident light beam, $E(t_x,t_y)$ is the irradiance produced by the output light beam at T; $|\mathrm{J}(\mathbf{T})|$ is the determinant of the Jacobian matrix of the position vector $\mathbf{T}$. Equation (2) is an elliptic Monge–Ampère equation which represents the conservation and redistribution of power during the beam-shaping process. From Eq. (2) we can see that the freeform surface is fully governed by $I(\theta, \varphi)$ and $E(t_x,t_y)$. That means we may need to redesign the freeform lens once either $I(\theta, \varphi)$ or $E(t_x,t_y)$ is changed.

The incident rays captured by the freeform transmitter can be grouped into two kinds of rays: the boundary rays and the inner rays. It is obvious that the propagation of the inner rays is fully governed by Eq. (2). For the boundary rays, the propagation of each ray should obey a boundary condition, which is defined as

$$\begin{cases} t_x = f(\theta, \varphi, \rho, \rho_\theta, \rho_\varphi) \\ t_y = g(\theta, \varphi, \rho, \rho_\theta, \rho_\varphi) \end{cases} : \partial\Omega_1 \rightarrow \partial\Omega_2 \tag{3}$$

where, $\partial \mathrm{W}_1$ and $\partial \mathrm{W}_2$ are the boundaries of Ω_1 and Ω_2 which are the domains on which $\mathrm{I}(\theta,\varphi)$ and $\mathrm{E}(t_x,t_y)$ are defined. Equation (3) tells us that the boundary rays are mapped onto the boundary of the illumination pattern after refraction by the freeform transmitter. From Eqs. (2) and (3) we can see that the tailoring of the freeform transmitter is fully governed by an elliptic Monge–Ampère equation with a nonlinear boundary condition. The exit surface is then obtained by numerically solving Eqs. (2) and (3), which are based on Newton's iteration [23].

2.2. Signal reception and processing

As illustrated in the Fig. 2, the camera receiver in the FreeOCC system captures the reflected modulated light from the observation plane and generates a series of frames with banded sections. Such banded sections (the RoIs) carry transmitted information to be decoded. Thanks to the uniform rectangular illumination produced by the freeform transmitter on the observation plane, the captured light signals have a relatively high and uniform SNR in the RoIs. Although the RoIs are visually straightforward to be recognized, it is far from trivial to extract them automatically by a smartphone. Refer to our previous work [10], we use Open Source Computer Vision (OpenCV) algorithm to extract the RoIs. A received frame first goes through a Gaussian blur and conducts a binary conversion to figure out the contour for extracting the RoIs [marked by the red rectangular box shown in Fig. 4(b)]. More details on RoIs extraction can be found in our previous work [10].

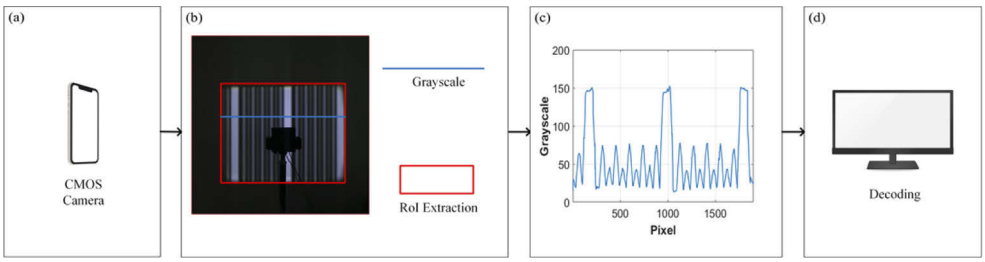

Fig. 4. The illustration of signal reception and decoding.

Given a RoI in the frame captured by the FreeOCC camera, only one row of pixels is selected out to form a grayscale sequence for decoding [marked by the blue line shown in Fig. 4(b)]. To

Optics EXPRESS

be more specific, we set a header to indicate the start of a packet, and the packet structure can be found in Section 3.1, due to the fact that the OCC is asynchronous and one-way communication. The header has the highest brightness and symbol width in a packet, as shown in Fig. 4(c). Thus, a rough threshold can be used to distinguish the headers in the RoI. Thanks to the uniform and sufficient SNR in FreeOCC, once all headers are located, the fine-grained thresholds are generated by using the headers' grayscale information to demodulate and decode out the bits between two adjacent headers, so that recovers the sent messages and completes the decoding procedure.

3. Experimental results and discussions

3.1. Prototype of the proposed FreeOCC system

In order to evaluate the performance of the proposed FreeOCC system, we build a prototype as shown in Fig. 5. In the freeform transmitter, a Xilinx XC7Z020 FPGA chip is used to generate the digitally controlled signal for light modulation. Here we employ 4-order and 8-order pulse amplitude modulations (4-PAM and 8-PAM) to generate various brightness levels to represent symbols and pack the sent symbols as a preamble of 4 successive brightest symbols under each order of PAM to indicate the header, followed by 19 data bits. The light source is a white LED chip with a size of 1.3 mm × 1.3 mm and works at a power supply of 2.05 watts which can emit an illuminance of 160 lux at a distance of 1 m. The freeform lens is designed by the Mong-Ampère equation method presented above. The freeform surface is shown in Fig. 6(a). The irradiance distribution produced by the freeform lens on the observation plane is shown in Fig. 6(b), and the normalized irradiance distributions along the lines x=0 mm and y=0 mm are given in Fig. 6(c). From Figs. 6(b) and 6(c) we can see a very good agreement between the actual irradiance distribution and the prescribed one. The freeform lens is further fabricated by injection moulding. The light rays from the LED light source are redirected by the freeform lens, producing a uniform rectangular illumination pattern on the observation plane with a size of 800 mm × 1000 mm, as shown in Fig. 7. We employ the HUAWEI P30's camera as the FreeOCC's receiver and configure the camera to work in the preview mode with a frame rate of 30 fps. The focal length of the camera is 35 mm that is fixed during all experiments, and the field of view of the camera equals 54.4°×37.8°. The camera's exposure time is set as 1/4000 s, and the camera's sensitivity (ISO) is set as 1500.

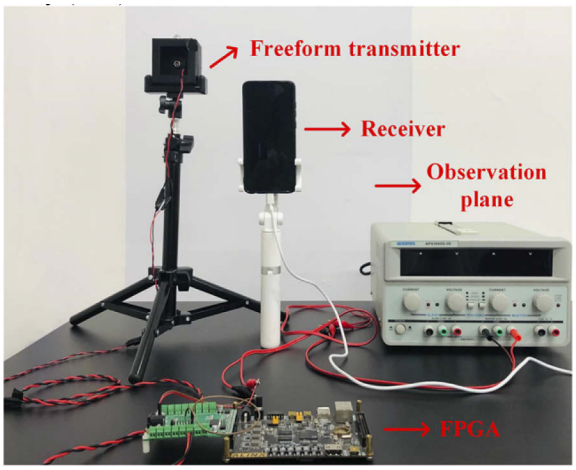

Fig. 5. Experimental setup of the proposed FreeOCC system.

Optics EXPRESS

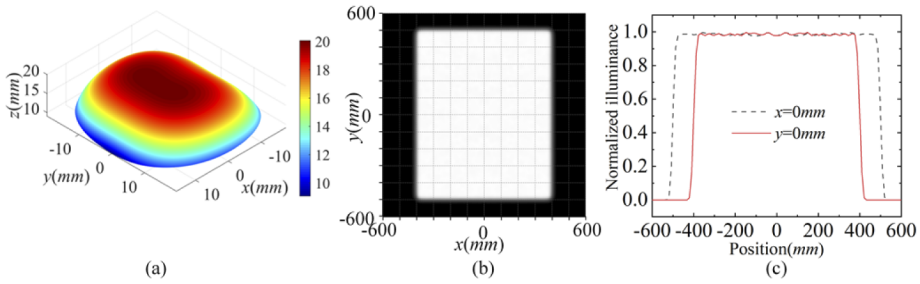

Fig. 6. Simulation results: (a) the freeform surface; (b) the illumination pattern on the observation plane; (c) the irradiance distributions along the lines x=0 mm and y=0 mm.

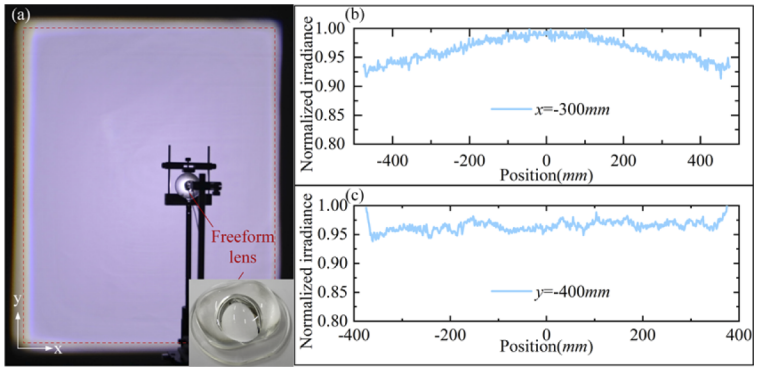

Fig. 7. (a) The freeform lens and the uniform rectangular illumination pattern; the irradiance distributions along the lines x = −300 mm (b) and y = −400 mm (c). The fractional RMS is employed here to quantify the illumination uniformity [24]. A smaller value of RMS represents better system performance. We have RMS = 0.0205 along the line x = −300 mm, and RMS = 0.0088 along the line y = −400 mm, indicating a high uniformity.

3.2. *Results and discussions*

In this section, we present the experimental results generated by the proposed FreeOCC system. Since it is necessary to consider the impact of the data rate and communication position in practical application scenarios, here we set three metrics to quantify the results of the experiments. The three metrics are transmission frequency, the distance between the observation plane and the receiver, and the receiver's viewing angle. A conventional reflected OCC system without the freeform lens is built as the baseline for comparison. We evaluate FreeOCC system in terms of *Packet Reception Ratio* (PRR) and *Bit Error Rate* (BER): while the former is the ratio between the successfully identified packets (those between two consecutive headers) and total transmitted ones, the latter represents the percentage of wrongly demodulated bits out of all successfully identified bits. 450 packets and more than 10000 bits are recorded in each test, and we report the average outcome over all experiments.

We first explore the proposed FreeOCC system performance in terms of PRR and BER under varying transmission frequencies. The freeform transmitter and receiver are, respectively, placed at a distance of 20 cm and 40 cm away from the observation plane. The viewing angle is set to be 0°. Figure 8 gives the changes of PRRs and BERs when the transmission frequencies are varied from 4 kHz to 6 kHz. The PRR increases with an increasing transmission frequency, due to the fact that symbol width is reduced at a higher frequency, and a RoI can carry more packets. In particular, the dedicatedly tailored freeform lens which produces a uniform rectangular

Optics EXPRESS

illumination on the observation plane, the uniformity of the grayscale distribution on a RoI is significantly improved, and the proposed FreeOCC system captures more valid symbols and completed packets within a frame than the baseline. Therefore, the PRR curve of FreeOCC outperforms the baseline under varying frequencies. For example, the PRRs are increased by 35% and 32% for 4-PAM and 8-PAM respectively, at a transmission frequency of 5 kHz. Similarly, the BER results of the FreeOCC system also significantly outperform the baseline, as shown in Figs. 8(b) and 8(c). The BERs are decreased by 72% and 59% for 4-PAM and 8-PAM, respectively, at the transmission frequency of 5 kHz. Moreover, the 4-PAM has a larger symbol distance than 8-PAM, so the PRR and BER of 4-PAM are slightly better than those of 8-PAM at a cost of a lower symbol-bit ratio. To enrich the presentation and help analyze more distinctly, we also display the constellation diagrams in the BER plots shown in Figs. 8(b) and 8(c). When the transmission frequency is changed from 4 kHz to 6 kHz, the BERs of the FreeOCC system are increased by 6.1% and 6.68%, respectively, for 4-PAM and 8-PAM, whereas the BERs results of baseline are increased by 9.9% and 10.98% respectively, and it again strongly confirms the effectiveness of the freeform lens in FreeOCC.

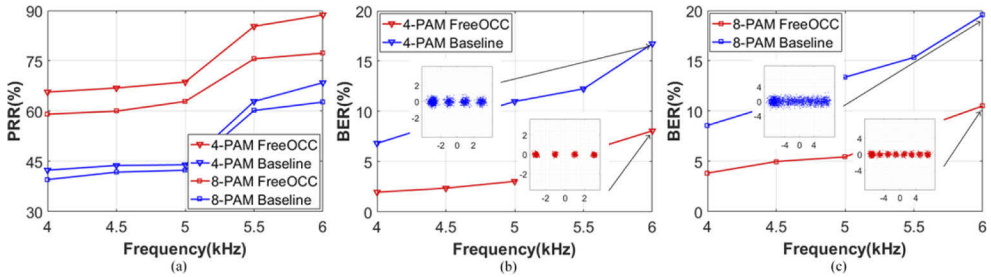

Fig. 8. Impact of various transmission frequencies on demodulation. (a) Packet reception rate; (b) Bit error rate of 4-PAM; (c) Bit error rate of 8-PAM.

In practical scenarios, the communication distance has a fundamental impact on the channel property. Thus, it is necessary to evaluate the performance of the proposed FreeOCC system at different distances between the observation plane and the receiver. The distance between the freeform transmitter and the observation plane remains unchanged. The viewing angle is set to be 0°, and the transmission frequency is configured at 4 kHz. Figure 9 depicts the change of the PRRs and BERs when the distance between the observation plane and the receiver is changed from 20 cm to 80 cm. As can be seen in Fig. 9, the greater the distance between the observation plane and the receiver, the severer the signal attenuation due to the focal length of camera is fixed, and the size of the RoI within the projected area is reducing. In the meantime, the RoI recorded by the receiver camera shrinks and gets vaguer, lowering the PRR. However, the PRR curves of FreeOCC system consistently outperform the baseline because of an increased SNR at the sides of the RoI enabled by the freeform lens. Similarly, the BER is increased due to the signal attenuation caused by a further distance. Nevertheless, the FreeOCC system still maintains a better performance than the baseline. Specifically, the BERs of FreeOCC system are only 1.38% and 3.20% respectively for 4-PAM and 8-PAM at 20 cm, which is over 73% and 53% less than the baseline, respectively. Additionally, the FreeOCC system still has relatively low BERs even at 80 cm, whereas the results of baseline are over 2 times more than the proposed FreeOCC system. Moreover, it is worth mentioning that the slope of the BERs curves of the FreeOCC system is obviously smaller than that of the baseline, which indicates the freeform lens contributes to alleviating the channel attenuation by precisely controlling the propagation of the modulated light. In a nutshell, the obtained experimental results clearly demonstrate that the freeform lens has the significant potential to improve the communication performance of current reflected OCC systems.

Optics EXPRESS

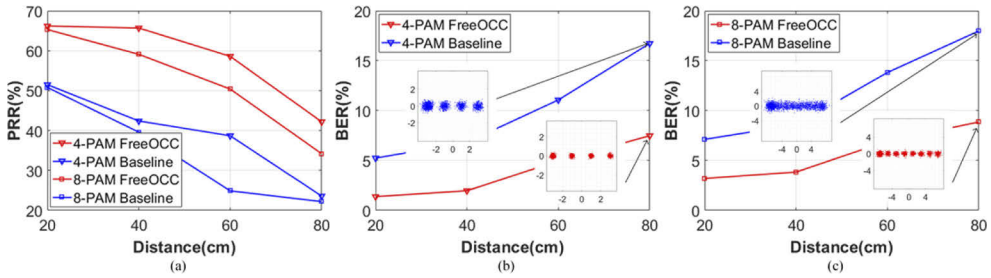

Fig. 9. Impact of various distances between observation plane and receiver on demodulation. (a) Packet reception rate; (b) Bit error rate of 4-PAM; (c) Bit error rate of 8-PAM.

In practical applications, since the receiver may not face the observation plane perpendicularly, inevitably the channel property of an OCC system will be influenced by the viewing angle. In this experiment, we examine the FreeOCC system performance under different viewing angles varying from $-60°$ to $60°$. The distance between the observation plane and the receiver still maintains 40 cm, and the other experiment settings remain unchanged. When the receiver is right pointing to the observation plane center at $0°$, the PRRs and BERs have the best results compared with other cases as illustrated in Fig. 10. Obviously, the PRRs and BERs are both degraded with the increasing of viewing angles due to the distorted RoIs that in turn affect the quality of the received grayscale symbols. Nevertheless, the PRRs and BERs performance of the FreeOCC system always maintain a better level comparing with the baseline, thanks to the uniform illumination pattern produced by the freeform transmitter in the FreeOCC system, yielding uniform and sufficient SNR in whole RoIs. Therefore, we can exactly conclude that FreeOCC system maintains a rather good channel quality within a wide viewing angle than the baseline.

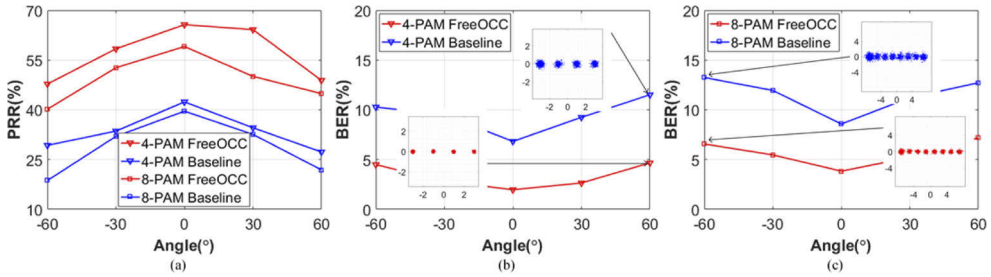

Fig. 10. Impact of various viewing angles on demodulation. (a) Packet reception rate; (b) Bit error rate of 4-PAM; (c) Bit error rate of 8-PAM.

4. Conclusions

To tackle the problems of unbalance and low SNR in the current reflected OCC systems, a FreeOCC system that employs a dedicatedly tailored freeform lens to precisely control the propagation of the modulated light is proposed in this paper. The freeform lens produces a prescribed uniform rectangular illumination on the observation plane so that the camera captures a uniform grayscale distribution in the received frames, and the SNR at the marginal region of RoI is significantly improved. To verify the effectiveness of the proposed system, we have fabricated the freeform lens and built a prototype for the proposed FreeOCC system. Based on the prototype, the performance of the proposed FreeOCC system is extensively evaluated in various experiment metrics. Two modulation schemes of 4-PAM and 8-PAM have been performed

Optics EXPRESS

on the prototype of the proposed FreeOCC system. The PRR is increased by 35% and 32%, respectively; meanwhile, the BER is decreased by 72% and 59%, respectively, at a transmission frequency of 5 kHz, comparing with the baseline. The results clearly show that the performance of a reflected OCC system can be dramatically improved by the use of a freeform lens and the proposed FreeOCC system significantly outperforms the conventional reflected OCC systems.

Funding. National Natural Science Foundation of China (NSFC) (11804299, 12074338, 61902267, 62002250, 62022071, 62072319); Fundamental Research Funds for the Central Universities (YJ201868); Applied Basic Research Program of Sichuan Province (2019YJ0110); Key Research and Development Program of Sichuan Province (2020YFS0575).

Disclosures. The authors declare no conflicts of interest.

Data availability. Data underlying the results presented in this paper are not publicly available at this time but may be obtained from the authors upon reasonable request.

References

1. N.-T. Le and Y and M. Jang, "MIMO architecture for optical camera communications," J. KICS. **42**(1), 8–13 (2017).
2. P. Luo, M. Zhang, H. L. Minh, H. M. Tsai, X. Tang, L. C. Png, and D. Han, "Experimental demonstration of RGB LED-based optical camera communications," IEEE Photonics J. **7**(5), 1–12 (2015).
3. J. Lain, Z. Yang, and T. Xu, "Experimental DCO-OFDM optical camera communication systems with a commercial smartphone camera," IEEE Photonics J. **11**(6), 1–13 (2019).
4. K. Mori, T. Takahashi, I. Ide, H. Murase, T. Miyahara, and Y. Tamatsu, "Recognition of foggy conditions by in-vehicle camera and millimeter wave radar," in *2007 IEEE Intelligent Vehicles Symposium* (2007), pp. 87–92.
5. Yehu Shen, U. Ozguner, K. Redmill, and J. Liu, "A robust video based traffic light detection algorithm for intelligent vehicles," in *2009 IEEE Intelligent Vehicles Symposium* (2009), pp. 521–526.
6. C. Danakis, M. Afgani, G. Povey, I. Underwood, and H. Haas, "Using a CMOS camera sensor for visible light communication," in *2012 IEEE Globecom Workshops* (2012), pp. 1244–1248.
7. H. Lee, H. Lin, Y. L. Wei, H. I. Wu, H. M. Tsai, and K. Lin, "RollingLight: Enabling line-of-sight light-to-camera communications," in *2015 Annual International Conference on Mobile Systems, Applications, and Services* (2015), pp. 167–180.
8. Y. Yang, J. Hao, and J. Luo, "CeilingTalk: Lightweight indoor broadcast through LED-camera communication," IEEE Trans. Mobile Comput. **16**(12), 3308–3319 (2017).
9. N. T. Le, M. A. Hossain, and Y. M. Jang, "A survey of design and implementation for optical camera communication," Signal Process. Image Commun. **53**, 95–109 (2017).
10. Y.-S. Kuo, P. Pannuto, K.-J. Hsiao, and P. Dutta, "Luxapose: Indoor positioning with mobile phones and visible light," in *20th Annual International Conference on Mobile Computing and Networking* (2014), pp. 447–458.
11. T. Yamazato, M. Kinoshita, S. Arai, E. Souke, T. Yendo, T. Fujii, K. Kamakura, and H. Okada, "Vehicle motion and pixel illumination modeling for image sensor based visible light communication," IEEE J. Sel. Areas Commun. **33**(9), 1793–1805 (2015).
12. H.-W. Chen, S.-S. Wen, Y. Liu, M. Fu, Z.-C. Weng, and M. Zhang, "Optical camera communication for mobile payments using an led panel light," Appl. Opt. **57**(19), 5288–5294 (2018).
13. G. P. Nava, H. D. Nguyen, Y. Kamamoto, T. G. Sato, Y. Shiraki, N. Harada, and T. Moriya, "A high-speed camera-based approach to massive sound sensing with optical wireless acoustic sensors," IEEE Trans. Comput. Imag. **1**(2), 126–139 (2015).
14. G. P. Nava, H. D. Nguyen, Y. Hioka, Y. Kamamoto, T. G. Sato, Y. Shiraki, and T. Moriya, "GPU-based real-time beamforming for large arrays of optical wireless acoustic sensors," Acoust. Sci. Technol. **36**(6), 489–499 (2015).
15. J. Hao, Y. Yang, and J. Luo, "CeilingCast: Energy efficient and location-bound broadcast through LED-camera communication," in *IEEE INFOCOM 2016 - The 5th Annual IEEE International Conference on Computer Communications* (2016), pp. 1–9.
16. Y. Yang, J. Nie, and J. Luo, "Reflexcode: Coding with superposed reflection light for LED-camera communication," in *23rd Annual International Conference on Mobile Computing and Networking* (2017), pp. 193–205.
17. C. Chow, C. Chen, and S. Chen, "Enhancement of signal performance in LED visible light communications using mobile phone camera," IEEE Photonics J. **7**(5), 1–7 (2015).
18. J. Lain, F. Jhan, and Z. Yang, "Non-Line-of-Sight optical camera communication in a heterogeneous reflective background," IEEE Photonics J. **11**(1), 1–8 (2019).
19. L. Liu, Y. Hong, and L. Chen, "A frame averaging based signal tracing (FAST) algorithm for optical camera communications," in *2018 Asia Communications and Photonics Conference (ACP)* (2018), paper Su3D.3.
20. K. Liang, C.-W. Chow, Y. Liu, and C.-H. Yeh, "Thresholding schemes for visible light communications with CMOS camera using entropy-based algorithms," Opt. Express **24**(22), 25641–25646 (2016).
21. Z. Zhang, T. Zhang, J. Zhou, Y. Lu, and Y. Qiao, "Thresholding scheme based on boundary pixels of stripes for visible light communication with mobile-phone camera," IEEE Access **6**, 53053–53061 (2018).
22. R. Wu, L. Yang, Z. Ding, L. Zhao, D. Wang, K. Li, F. Wu, Y. Li, Z. Zheng, and X. Liu, "Precise light control in highly tilted geometry by freeform illumination optics," Opt. Lett. **44**(11), 2887–2890 (2019).

Optics EXPRESS

23. R. Wu, P. Liu, Y. Zhang, Z. Zheng, H. Li, and X. Liu, "A mathematical model of the single freeform surface design for collimated beam shaping," Opt. Express **21**(18), 20974–20989 (2013).
24. L. Yang, Y. Liu, Z. Ding, J. Zhang, X. Tao, Z. Zheng, and R. Wu, "Design of freeform lenses for illuminating hard-to-reach areas through a light-guiding system," Opt. Express **28**(25), 38155–38168 (2020).